Journal of Zhejiang University-SCIENCE C (Computers & Electronics)
ISSN 1869-1951 (Print); ISSN 1869-196X (Online)
www.zju.edu.cn/jzus; www.springerlink.com
E-mail: jzus@zju.edu.cn

Optimized simulated annealing algorithm for thinning and weighting large planar arrays*

Peng CHEN[†1], Bin-jian SHEN[2], Li-sheng ZHOU[2], Yao-wu CHEN[†‡1]

([1]*Institute of Advanced Digital Technologies and Instrumentation, Zhejiang University, Hangzhou 310027, China*)

([2]*Hangzhou Applied Acoustics Research Institute, Hangzhou 310012, China*)

[†]E-mail: chenpeng123@zju.edu.cn; cyw@mail.bme.zju.edu.cn

Received Jan. 15, 2009; Revision accepted Apr. 27, 2009; Crosschecked Nov. 30, 2009

Abstract: This paper proposes an optimized simulated annealing (SA) algorithm for thinning and weighting large planar arrays in 3D underwater sonar imaging systems. The optimized algorithm has been developed for use in designing a 2D planar array (a rectangular grid with a circular boundary) with a fixed side-lobe peak and a fixed current taper ratio under a narrow-band excitation. Four extensions of the SA algorithm and the procedure for the optimized SA algorithm are described. Two examples of planar arrays are used to assess the efficiency of the optimized method. The proposed method achieves a similar beam pattern performance with fewer active transducers and faster convergence ability than previous SA algorithms.

Key words: Simulated annealing (SA), Sparse planar arrays, 3D underwater sonar imaging, Beam pattern, Optimization
doi:10.1631/jzus.C0910037 **Document code:** A **CLC number:** TB56

1 Introduction

In the process of thinning and weighting a large planar array some transducers need to be turned off and some weighting parameters changed in an evenly spaced or periodic array to minimize the number of active transducers and to obtain a fixed side-lobe peak (SLP) and a fixed current taper ratio (CTR) (the ratio between the maximum and minimum weight coefficient). Simulated annealing (SA) (Kirkpatrick *et al.*, 1983) and genetic algorithms (Haupt, 1994) are optimization methods that are well suited for thinning arrays. SA models the annealing (slow cooling) process of metals from a liquid to a solid state while genetic algorithms model evolution and genetic recombination in nature. Arrays that are thinned by SA algorithms (Kirkebo and Austeng, 2008; Trucco *et al.*, 2008) and genetic algorithms (Chen *et al.*, 2007; Haupt, 2007; 2008; Spence and Werner, 2008) have also been reported. Genetic algorithms are generally limited to the optimization of moderately sized arrays because of the large number of genes in large planar arrays. This paper focuses on optimizing an SA algorithm for thinning and weighting a large planar array.

Large arrays are needed for high-resolution 3D sonar systems to receive the back-scattered sonar signals in response to the insonification of a scene with a narrow band pulse (Palmese *et al.*, 2006). 3D real time acoustical imaging systems have been used extensively in applications including underwater construction, research, environmental studies, survey of shipwrecks, dredging, offshore oil detection, and military applications (Davis and Lugsdin, 2005; Hansen *et al.*, 2005). To prevent grating lobes, a half-wavelength ($\lambda/2$) spacing between the transducers of the array should not be exceeded. At the same time, the array should have a wide spatial extension to obtain a fine lateral resolution. The $\lambda/2$-condition with the fine resolution requirement often results in a 2D array composed of some

‡ Corresponding author

* Project (No. 2006AA09Z109) supported by the National High-Tech Research and Development Program (863) of China

thousands of transducers (Trucco, 1999; Trucco *et al.*, 2008). Critical issues in the development of high-resolution 3D sonar systems are (1) the cost of hardware associated with the huge number of sensors that comprise the planar array, and (2) the computational burden in processing the signals (Trucco *et al.*, 2008). An algorithm is proposed to perform chirp zeta transform (CZT) beamforming on the wideband signals collected by an evenly spaced planar array and generated by a scene placed in both the far-field (Palmese and Trucco, 2007a) and the near-field (Palmese and Trucco, 2007b).

Trucco *et al.* (2008) provided new information on the development of an advantageous and affordable sparse planar array for high-resolution real-time underwater imaging systems, in which the positions and weights of the array transducers are optimized simultaneously. Note that the best result reported achieves an SLP of −22 dB and a CTR of 3.28 with 584 transducers. Our method achieves a better result than previous methods (Trucco, 1999; Trucco *et al.*, 2008) when four extensions are added to the SA: (1) The weights of the whole array transducers are initialized with random values; (2) The 'energy' function is redefined; (3) The death and resurrection probabilities are also redefined; (4) The termination criterion is defined.

2 Four extensions to simulated annealing

SA was initially developed to simulate the behavior of the molecules of a pure substance during the slow cooling that results in the formation of a perfect crystal (minimum energy state) (Kirkpatrick *et al.*, 1983). It is a stochastic methodology to solve multi-objective optimization problems. The algorithm is iterative: in each new iteration, a small random perturbation is induced. If the new configuration causes the value of the energy function to decrease, it is accepted as a new optimal state. Conversely, if the new configuration increases the value of the energy, it is accepted with a probability depending on the system temperature, in accordance with the Boltzmann distribution (Trucco, 1999). The higher the temperature, the higher the probability of the state configuration which causes the energy configuration to increase; it may then be accepted as the new configuration. As iterations continue, the temperature is gradually lowered until the configuration 'freezes' to a certain final state.

The objective array is an evenly spaced planar array (a rectangular grid with a circular boundary) on the plane (z=0) consisting of $M\times N$ rectangular grids (usually M=N). The far-field beam pattern (BP) (Nielsen, 1991) can be presented as

$$b(\boldsymbol{W}, \boldsymbol{u}) = \left| \sum_{m=1}^{M} \sum_{n=1}^{N} \omega_{m,n} \exp\left(\mathrm{j} \frac{2\pi}{\lambda} \cdot \boldsymbol{r}_{m,n} \cdot (\boldsymbol{v} - \boldsymbol{u}) \right) \right|, \quad (1)$$

where $\boldsymbol{v}$ is the unit-direction vector which is perpendicular to the plane wave, $\boldsymbol{W}$ is the array of the weights $\omega_{m,n}$ that are applied to control the SLP, $\boldsymbol{u}$ is the unit vector of the steering direction, λ is the wavelength of the backscattered echoes, and $\boldsymbol{r}_{m,n}$ denotes the vector of the sensor coordinate identified by the indexes presented as

$$\boldsymbol{r}_{m,n}=((m-(M+1)/2)d, (n-(N+1)/2)d), \quad (2)$$

where $1\le m\le M$, $1\le n\le N$, and d is the distance between two adjacent transducers along the x axis and along the y axis. The unit vector $\boldsymbol{u}$ (van Trees, 2002) can be expressed as

$$\begin{cases} \boldsymbol{u} = (u_x, u_y, u_z) = (\sin\theta\cos\varphi, \sin\theta\sin\varphi, \cos\theta), \\ u_x \in [-1,\ 1],\ u_y \in [-1,\ 1], \end{cases} \quad (3)$$

where φ is the azimuth angle and θ is the elevation angle. $\boldsymbol{v}$=(0, 0, 1) is set as described in the plane array BP of van Trees (2002). Substituting Eq. (2) and Eq. (3) in Eq. (1) gives

$$b(\boldsymbol{W}, u_x, u_y) = \left| \sum_{m=1}^{M} \sum_{n=1}^{N} \omega_{m,n} \exp\left(\mathrm{j} \frac{2\pi d}{\lambda} \left(\left(\frac{M+1}{2} - m \right) u_x + \left(\frac{N+1}{2} - n \right) u_y \right) \right) \right|, \quad (4)$$

where

$$\begin{cases} b(\boldsymbol{W}, u_x, u_y) = b(\boldsymbol{W}, -u_x, u_y), \\ b(\boldsymbol{W}, u_x, u_y) = b(\boldsymbol{W}, u_x, -u_y). \end{cases} \quad (5)$$

Because of the symmetry properties shown in Eq. (5), the value ranges of u_x and u_y can be restricted to

$u_x \in [0, 1]$, $u_y \in [0, 1]$ in analyzing the performance of the BP. The expression in decibels for the power output of the BP is given as

$$\boldsymbol{P}(\boldsymbol{W}, u_x, u_y) = 10 \times \lg b^2(\boldsymbol{W}, u_x, u_y). \quad (6)$$

For convenience in comparing the results from this and other methods (Trucco, 1999; Trucco *et al.*, 2008), the expression for analyzing performances for the BP normalized to 0 dB, is given as

$$\mathrm{BP}(\boldsymbol{W}, u_x, u_y) = 20 \times \lg \frac{b(\boldsymbol{W}, u_x, u_y)}{\max\left(b(\boldsymbol{W}, u_x, u_y)\right)}. \quad (7)$$

The four extensions to the SA (Trucco, 1999; Trucco *et al.*, 2008) are described in the following sections.

2.1 Extension 1: initial weight values

The initial weight values for the whole array transducers are represented by

$$\boldsymbol{W} = \begin{bmatrix} \omega_{1,1} & \omega_{1,2} & \cdots & \omega_{1,N} \\ \omega_{2,1} & \omega_{2,2} & \cdots & \omega_{2,N} \\ \vdots & \vdots & & \vdots \\ \omega_{M,1} & \omega_{M,2} & \cdots & \omega_{M,N} \end{bmatrix}, \quad (8)$$

where $\omega_{m,n}$=0 or 1 ($1 \le m \le M$, $1 \le n \le N$). These values are created initially by a random number generator with 0 or 1, and the weight values that are out of the circular boundary are always set to zero during the optimization procedure. If the weight value $\omega_{m,n}$ is not equal to 0, it means that the indexes (m, n) transducer is active. The location of this active transducer is also fixed. If all of the weight values were accessed, the number of total active transducers would also be determined. Thus, the optimization procedure for thinning and weighting whole planar arrays is the procedure for choosing the weight values. This is different from the method of Trucco *et al.* (2008) where the symmetry of the sparse array layout around the x and y axes is utilized, and only a quarter of the array transducers are used in the optimization procedure. Optimizing the whole array will reduce the number of active transducers in the array compared with optimizing only a quarter of the array transducers. This extension also makes the SA algorithm converge faster compared with having all 1s or all 0s in the initial weight values.

2.2 Extension 2: redefinition of the energy function

The aim of the optimization procedure is to determine the weight values that make the energy function freeze to the lowest state. The energy function or the cost function contains all the objectives' parameters. The weight of each factor can be decided by its weight factor. The objective of thinning and weighting the large planar arrays in this paper is to minimize the number of active transducers and to satisfy a fixed SLP and CTR. Thus, the energy function that contains the three terms can be shown as

$$E(\boldsymbol{W}, A) = k_1 \left(\sum_{(u_x, u_y) \in \Omega} \left(\frac{b(\boldsymbol{W}, u_x, u_y)}{B} - b_\mathrm{d}(u_x, u_y) \right) \right)^2 + k_2 A^2 + k_3 (R_\mathrm{o} - R_\mathrm{d})^2, \quad (9)$$

$$B = \max\left(b(\boldsymbol{W}, u_x, u_y)\right), \quad (10)$$

where A is the number of active transducers, k_1, k_2 and k_3 are the weight factors for each term, R_o and R_d denote the obtained and desired CTR values respectively, $b_\mathrm{d}(u_x, u_y)$ denotes the desired SLP, and Ω is the set of values (u_x, u_y) which satisfies

$$u_x^2 + u_y^2 > \lambda / D, \quad (11)$$

$$\frac{b(\boldsymbol{W}, u_x, u_y)}{B} > b_\mathrm{d}(u_x, u_y), \quad (12)$$

where D is the diameter of the circular boundary. The main lobe is excluded from the validity region. The Ω, which is a set of discrete data, constrains the (u_x, u_y) to $u_x \in [0, 1/P, \ldots, p/P, \ldots, 1]$, $p \in [0, P]$ and $u_y \in [0, 1/Q, \ldots, q/Q, \ldots, 1]$, $q \in [0, Q]$. P and Q are two constants, because the maximum number of beams to be formed is a constant for each particular 3D underwater sonar imaging system. These three weight factors (k_1, k_2 and k_3) can vary in different 3D sonar systems. To avoid the third term playing a passive function in Eq. (9), it should be assigned to zero when $R_\mathrm{o} < R_\mathrm{d}$. This extension enables the optimized SA to achieve a similar BP performance with fewer active transducers compared with other published SA methods (Trucco, 1999; Trucco *et al.*, 2008) where P and Q are continuous data streams.

2.3 Extension 3: redefinition of the death and resurrection probabilities

During the optimization procedure, if the chosen transducer is active, it can be changed to inactive by following a death probability, whereas if the chosen transducer is inactive, it can be activated by following a resurrection probability (Trucco, 1999). Trucco (1999) and Trucco *et al.* (2008) gave a fixed death probability (Pr(death)=0.2) and a fixed resurrection probability (Pr(resurrection)=0.4). To achieve a similar BP performance with fewer active transducers compared with these methods, a variable resurrection probability and a fixed value for the death probability are redefined in this paper. The $((m-(M-1)/2)d, (n-(N-1)/2)d)$ coordinates are identified by the indexes (m, n) transducer, and the death and resurrection probabilities for the transducer are redefined as

$$\begin{cases} \Pr(\text{death}) = 1, \\ \Pr(\text{resurrection}) = \\ \quad k_4 \cdot \left(1 - \dfrac{4}{M \times N}\left(m - \dfrac{M-1}{2}\right)\left(n - \dfrac{N-1}{2}\right)\right), \end{cases} \tag{13}$$

where k_4 is a weight factor. Thus, if the chosen transducer is active, it would be changed to inactive. The state of the chosen transducer will be retained if the energy function is reduced by this variation. Otherwise, the inactive transducer will be reactivated and perturbed. The resurrection probability is higher at the center of the array and decreases toward the edges. Thus, the transducer density is the greatest at the center of the array and gradually decreases toward the edges. The side-lobes close to the main beam decrease while those far from the main beam increase, which is usually quite acceptable (Haupt, 2008).

2.4 Extension 4: termination criterion

Published methods (Trucco, 1999; Trucco *et al.*, 2008) do not include any termination criteria, but contain a large number of iterations. One of the main objectives of the optimization is to minimize the number of active transducers; if the active transducers A do not decrease in the last L iterations, it should be set as the termination criterion. If $A(l)$ denotes the number of active transducers after l iterations, then the termination criterion is given as

$$A(l-L+1)==A(l),\ \ l>L-1. \tag{14}$$

Thus, the minimum number of iterations is larger than $L-1$. After many runs of the proposed algorithm, L is set to 100. When $l>99$ and $A(l-99)==A(l)$, the iteration terminates. However, the greater is the number of iterations, the more stable is the system performance. L could be set as a number greater than 100 when a more critical stable system performance is required.

3 Optimized simulated annealing algorithm procedure

The optimized procedure is started by considering a fully sampled array, where D is the diameter of the received array, and the weight values which are out of the circular boundary are always set to zero. The objective of the procedure is to minimize the number of active transducers in the fully sampled array satisfying a desired CTR and SLP. A flow chart of the optimization procedure based on Trucco (1999) and Trucco *et al.* (2008) is shown in Fig. 1, where the round(), rand(), and unifrnd() are Matlab (MathWorks Inc., 2008) math functions. The procedures shown in Fig. 1 are described as follows:

1. The T_{start} and the weight values $\boldsymbol{W}$ are initialized. The initial temperature T_{start} is chosen high enough so that the first configuration perturbation will be almost always accepted, even though it leads to a sharp increase in the energy function (Trucco, 1999). The weight values $\boldsymbol{W}$ are initialized with random values of 0 or 1. This initialization will reduce the iteration number compared with assigning all 1s or all 0s to the weight values $\boldsymbol{W}$.

2. Choose a random transducer weight value $\omega_{m,n}$ and assign $\omega_{m,n}$ to ω_t. At each iteration, all the transducers are visited according to a random sequence that does not re-visit the same transducer before all others have been visited once.

(1) If the chosen transducer is inactive, it can be activated by the resurrection probability defined in Eq. (13). If the resurrection probability is larger than a random uniformly distributed number, a random weight value is assigned to the chosen transducer and the weight values $\boldsymbol{W}$ are updated. Otherwise, it goes to Step 2.

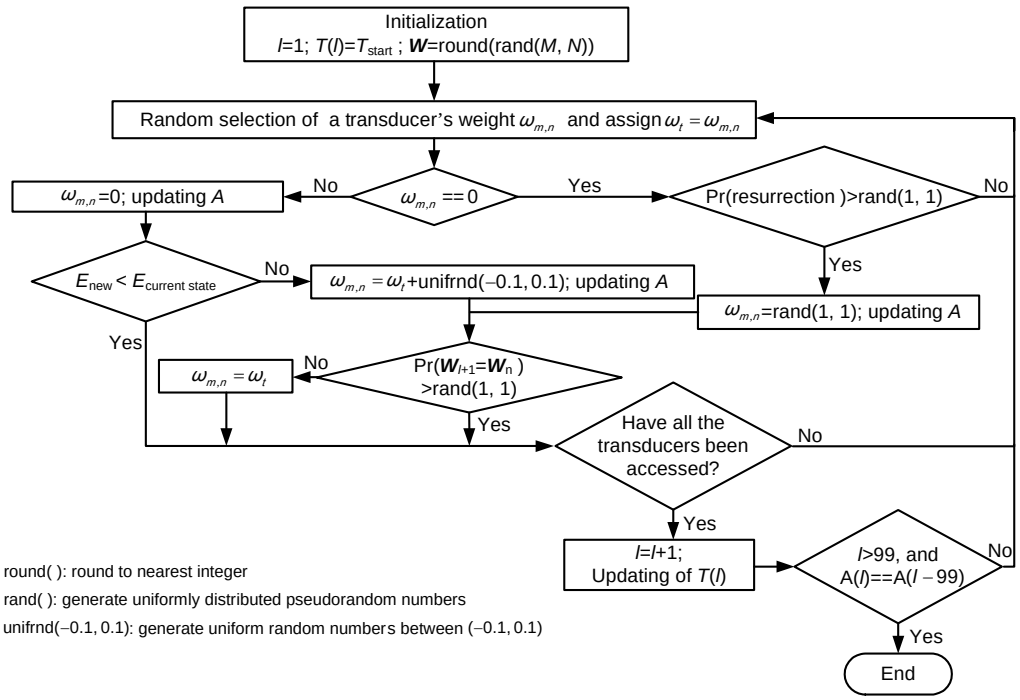

Fig. 1 Flow chart of the optimized simulated annealing

(2) If the chosen transducer is active, it always changes to inactive and the weight values $\boldsymbol{W}$ are updated. The inactive state of the chosen transducer will be retained when the energy function is reduced by this variation; then go to Step 3. Otherwise, the inactive transducer would be reactivated and perturbed.

(3) If the new weight $\boldsymbol{W}_{\mathrm{n}}$ decreases the value of the 'energy' function, it will be accepted as the next weight $\boldsymbol{W}_{l+1}$. If it increases this function, it will be accepted or restored as the weight value ω_t with a probability that depends on the 'temperature' of the system; the higher the temperature, the greater the probability of accepting a higher value of the 'energy' function. According to Kirkpatrick *et al*. (1983) the probability can be expressed as

$$\Pr(\boldsymbol{W}_{l+1}=\boldsymbol{W}_n)=\begin{cases}\exp\left(\dfrac{E_l-E_{\mathrm{n}}}{kT}\right), & \text{if } E_{\mathrm{n}}>E_l,\\ 1, & \text{otherwise,}\end{cases} \tag{15}$$

where E_l is the energy function in the lth iteration, E_{n} is new state energy, k is the Boltzmann constant, and T is the system temperature.

3. If all transducers have been accessed, update the iteration number l and the system temperature function $T(l)$, where

$$T(l)=\begin{cases}T_{\mathrm{start}}, & l=1,\\ 0.85\times T(l-1), & l>1;\end{cases} \tag{16}$$

otherwise the optimization goes to Step 2.

4. If the iteration procedure satisfies the termination criterion defined in Eq. (14), the optimization will terminate; otherwise it goes to Step 2.

4 Design of a thinned array

To assess the efficiency of the method, two tests were performed for verifying that the optimized SA is able to obtain a similar BP performance with fewer active transducers than other published SA (Trucco, 1999; Trucco *et al.*, 2008).

4.1 A 64×64 transducer array

The first test involved thinning a 64×64 rectangular grid planar array with a $\lambda/2$ inter-transducer spacing as described by Trucco (1999), where 359 active transducers achieve an SLP=−21.2 dB, a main-lobe width (measured at −6 dB) of 0.048, and a CTR of 3.1. In the optimization procedure, $b_{\mathrm{d}}(u_x, u_y)$ was set at 0.087 09 (20×lg 0.087 09≈−21.2 dB). The other parameters were fixed as follows: T_{start}=1000,

k_1=10 000, k_2=0.20, k_3=0.01, k_4=0.8, and R_d=3.1. In the u_x-u_y space ($u_x \in [0, 1]$, $u_y \in [0, 1]$), the number of beams' intensity to be calculated was 100×100. The radius for the each pair (u_x, u_y) excluding the main-lobe was $\lambda/D \approx 0.032$. After several runs of the proposed SA, the best results were obtained. Comparisons of the best results obtained by the optimized SA and by the method of Trucco (1999) are shown in Table 1, where R_o=3.0 and $R_o < R_d$. Thus, k_3 was assigned to zero at the end of the optimization. The optimized algorithm achieved a similar BP performance and a lower CTR value with fewer iterations and fewer active transducers than the previous published method. Defining R_a as the thinning ratio of the active transducers which achieve similar BP performances in this paper and in the literature, then

$$R_a = \frac{\text{Number of active transducers in optimized SA}}{\text{Number of active transducers in previous published SA}}. \quad (17)$$

Thus, R_a equaled about 71% in this thinning example. The power output for the BP is shown in Fig. 2, where the power output for the BP in direction of the signal ((u_x, u_y)=(0, 0)) is about 48.2 dB. Fig. 3 shows the normalized BP defined in Eq. (7) with an SLP of −21.2 dB. Fig. 4 shows the optimized layout of transducers, weight values of the optimized transducers and the number of active transducers versus the number of iterations. The active transducers' positions are shown as dots in Fig. 4a, the maximum and minimum weight values for the active transducers in Fig. 4b are about 1.72 and 0.57 respectively, and the number of active transducers in Fig. 4c shows a rapid descent slope during the first phase (from iteration 1 to about iteration 20) and is quasi-constant during the second phase (from about iteration 20 to iteration 154).

Table 1 Comparisons of the thinning results between the method of Trucco (1999) and ours

Method	N_a	$\max_{SLP}$ (dB)	CTR	MLW	N_i
Trucco (1999)	359	−21.2	3.1	0.048	1000
Ours	255	−21.2	3.0	0.048	154

N_a: number of active transducers; N_i: number of iterations; $\max_{SLP}$: maximum side-lobe peak; MLW: main-lobe width; CTR: current taper ratio

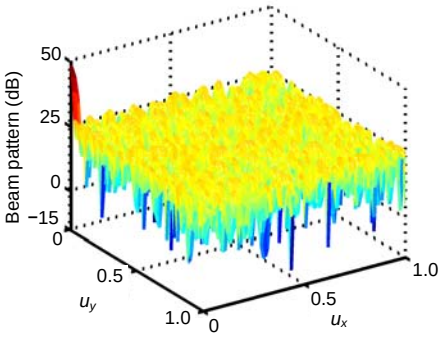

Fig. 2 Power output for the beam pattern of the 255 transducers

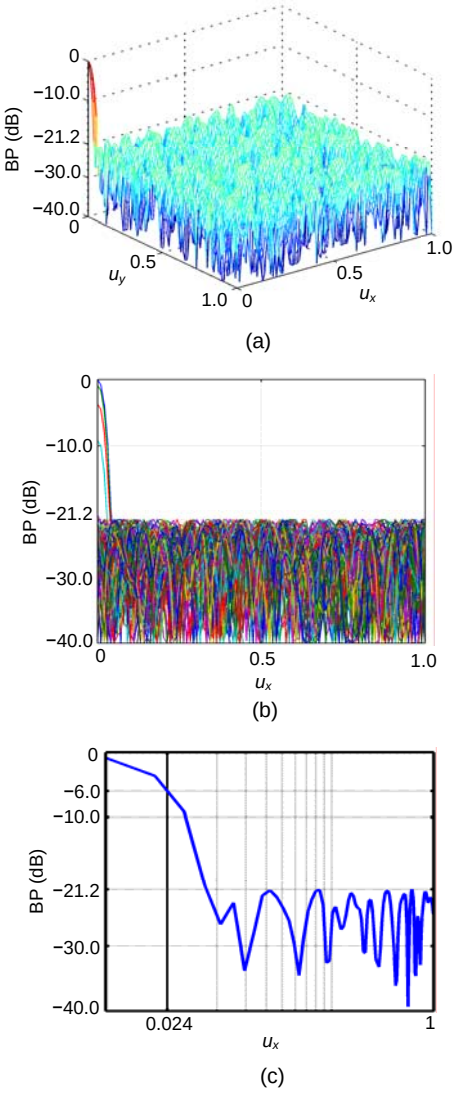

Fig. 3 (a) Normalized beam pattern with a side-lobe peak of −21.2 dB; (b) Side view of (a) integration along u_y; (c) Cut view of (a) at u_y=0 with logarithmic scale in u_x

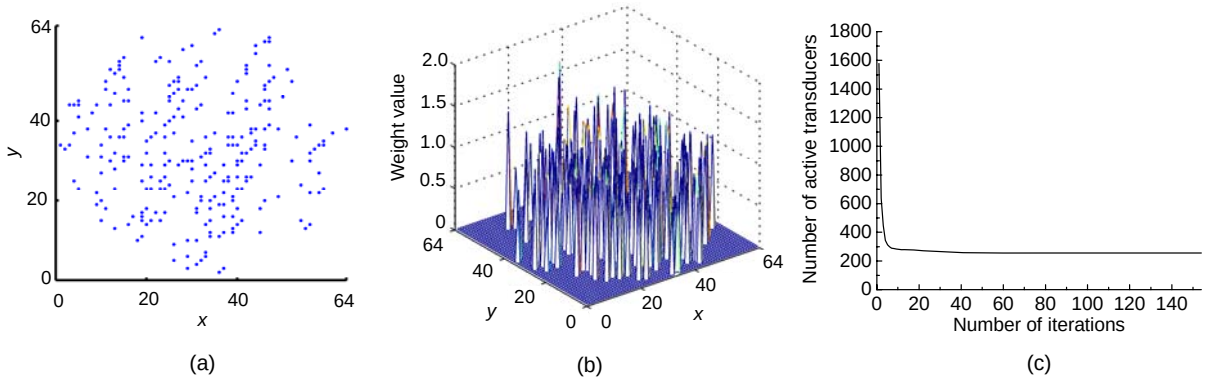

Fig. 4 (a) Optimized layout of a 255 transducers; (b) Weight values of the optimized transducers; (c) The number of active transducers versus the number of iterations

4.2 A 100×100 transducer array

In the second test we considered a 100×100 rectangular grid planar array with a $\lambda/2$ inter-transducer spacing. In Trucco *et al.* (2008), a maximum value of SLP equal to −22 dB and a CTR of 3.28 with 584 transducers were achieved. Thus, the parameters in the optimized SA were set as follows: $b_d(u_x, u_y)$=0.079 34 (20×lg 0.079 34≈−22 dB) and R_d=3.28. The other parameters were fixed as follows: T_{start}=1000, k_1=10 000, k_2=0.4, k_3=0.02, k_4=0.8, and the center frequency for the backscattered echoes was 300 kHz. The radius of each pair (u_x, u_y) excluding the main-lobe was λ/D=0.02. In the u_x-u_y space ($u_x \in [0, 1]$, $u_y \in [0, 1]$), the number of beams' intensity to be calculated was 200×200. After several runs of the proposed SA, the best results were obtained. Comparisons of the best results from this method and that of Trucco *et al.* (2008) are given in Table 2, where R_o=2.75 and $R_o < R_d$. Thus, k_3 was assigned to zero at the end of the optimization. The optimized planar array with fewer active transducers and a lower CTR achieved a similar BP performance compared with 584 active transducers reported by Trucco *et al.* (2008). The validity ranges of the view field were enlarged by 8° and 3°, respectively. The R_a was about 69% in this thinning example. The power output for the BP is shown in Fig. 5, where the power output for the BP in direction of the signal ((u_x, u_y)=(0, 0)) is about 52.0 dB. Fig. 6 shows the normalized BP defined in Eq. (7) with an SLP of −22 dB. Fig. 7 shows the optimized layout of transducers, weight values of the optimized transducers and the number of active transducers versus the number of iterations. The maximum and minimum weight values for the active transducers (Fig. 7b) are about 1.59 and 0.58, respectively. The number of active transducers in Fig. 7c shows a rapid descent slope during the first phase (from iteration 1 to about iteration 20) and is quasi-constant during the second phase (from about iteration 20 to iteration 151). The optimized array

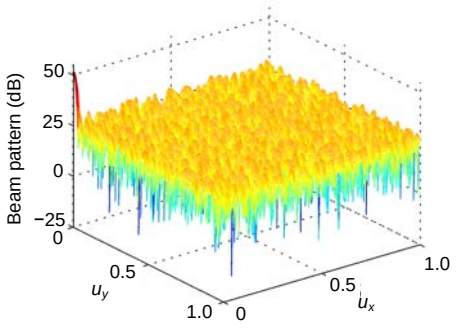

Fig. 5 Power output for the beam pattern of the 403 transducers

Table 2 Comparisons of the thinning results between the method of Trucco *et al.* (2008) and ours

Method	N_a	$\max_{SLP}$ (dB)	CTR	Angular resolution (°)		Field of view		N_i
				600 kHz, $d=\lambda$	1.2 MHz, $d=2\lambda$	600 kHz, $d=\lambda$	1.2 MHz, $d=2\lambda$	
Trucco *et al.* (2008)	584	−22	3.28	0.64	0.32	52°×52°	26°×26°	
Ours	403	−22	2.75	0.64	0.32	60°×60°	29°×29°	151

N_a: number of active transducers; N_i: number of iterations; $\max_{SLP}$: maximum side-lobe peak; CTR: current taper ratio

achieved a similar angular resolution (measured at −3 dB) to the resolution achieved by 584 active transducers in Trucco *et al.* (2008), where the inter-element spacing was equal to λ or 2λ. The angular resolutions are shown in Fig. 8, where $2\arcsin 0.0056 \approx 0.64°$, $2\arcsin 0.0028 \approx 0.32°$, and the field view ranges are 60°×60° ($2\arcsin 0.5 = 60°$) and 29°×29° ($2\arcsin 0.25 \approx 29°$), respectively.

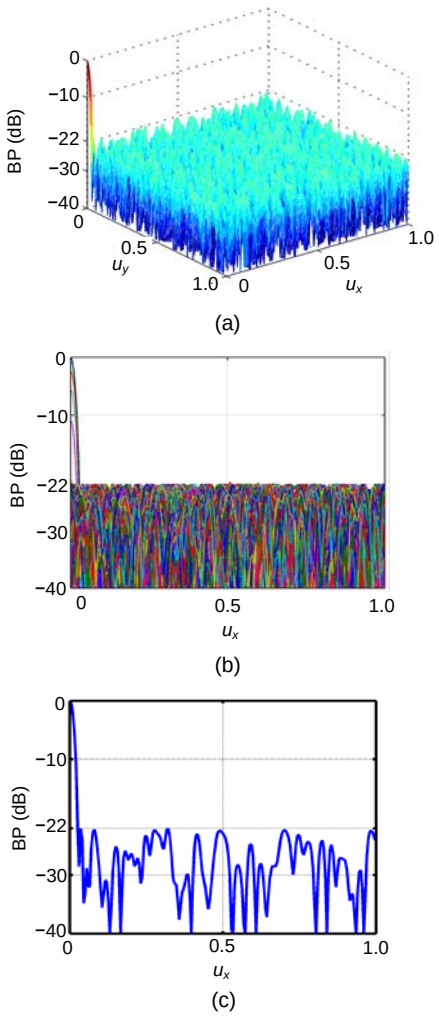

Fig. 6 (a) Normalized beam pattern with a side-lobe peak of −22dB; (b) Side view of (a) integration along u_y; (c) Cut view of (a) at u_y=0

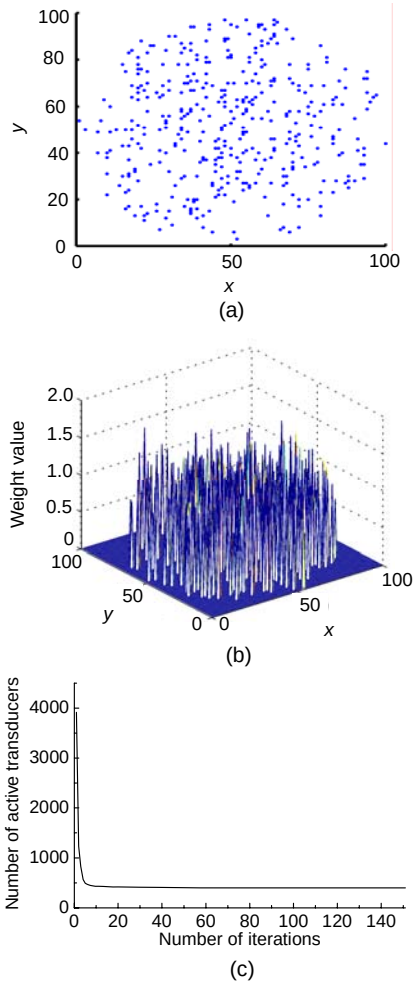

Fig. 7 (a) Optimized layout of 403 transducers; (b) Weight values of the optimized transducers; (c) The number of active transducers versus the number of iterations

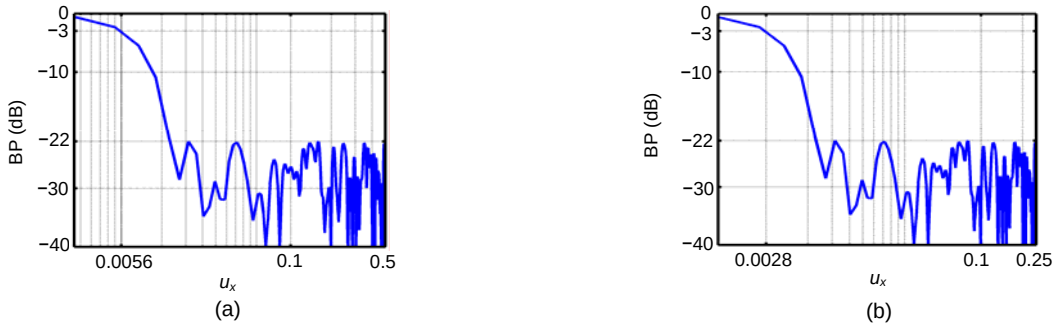

Fig. 8 (a) Inter-element spacing is equal to λ with logarithmic scale in u_x; (b) Inter-element spacing is equal to 2λ with logarithmic scale in u_x

5 Discussion

One of the main drawbacks in thinning operations is the high level of SLP. The optimized SA can constrain the SLP to a fixed level. The number of active transducers, the locations of the active transducers and the values of the transducers' weights determine the level of the side-lobes. To reduce the number of active transducers, the main aim in thinning a planar array is to increase the side-lobe levels which are far from the main-lobe. As all the side-lobe levels which are below the maximum SLP will be filtered out in the 3D sonar imaging system, these side-lobes have a wide tolerance range.

The four factors (k_1, k_2, k_3, k_4) play an important role in the optimization procedure. The number of direction beams has a great effect on the value of the three factors in Eq. (9). In the run experiments, the greater the number of direction beams, the higher the values of k_2 and k_3 need to be set or the lower value of k_1 needs to be set. In a thinned array, the exact SLP of the BP is hard to calculate, but an adequate number of beam directions could approach the exact SLP. In a real 3D sonar system, the maximum number of direction beams is fixed; if the CTR were not critically required in the system parameter, then the value of k_3 could be set to zero.

6 Conclusion

This paper confirms that the optimized SA can achieve a similar BP performance with fewer active transducers compared with other published SA. In two test examples, the proposed method achieved a thinning ratio for active transducers (R_a) of 71% and 69%, respectively. The paper also showed that the optimized SA has a faster convergence ability. The thinned planar array uses many fewer active transducers to gain a fixed SLP and a fixed CTR. As a result, the costs of the planar array and the signal computation burden are reduced.

References

Chen, K., Yun, X., He, Z., Han, C., 2007. Synthesis of sparse planar arrays using modified real genetic algorithm. *IEEE Trans. Antenn. Propag.*, **55**(4):1067-1073. [doi:10.1109/TAP.2007.893375]

Davis, A., Lugsdin, A., 2005. High Speed Underwater Inspection for Port and Harbour Security Using Coda Echoscope 3D Sonar. Proc. MTS/IEEE Oceans, p.2006-2011. [doi:10.1109/OCEANS.2005.1640053]

Hansen, R.K., Castellani, U., Murino, V., Fusiello, A., Puppo, E., Papaleo, L., Pittore, M., Gobbi, M., Bisone, L., Kleppe, K., *et al*., 2005. Mosaicing of 3D Sonar Data Sets: Techniques and Applications. Proc. MTS/IEEE Oceans, p.2326-2333. [doi:10.1109/OCEANS.2005.1640112]

Haupt, R.L., 1994. Thinned arrays using genetic algorithms. *IEEE Trans. Antenn. Propag.*, **42**(7):993-999. [doi:10.1109/8.299602]

Haupt, R.L., 2007. Optimized weighting of uniform subarrays of unequal sizes. *IEEE Trans. Antenn. Propag.*, **55**(4):1207-1210. [doi:10.1109/TAP.2007.893406]

Haupt, R.L., 2008. Optimized element spacing for low sidelobe concentric ring arrays. *IEEE Trans. Antenn. Propag.*, **56**(1):266-268. [doi:10.1109/TAP.2007.913176]

Kirkebo, J.E., Austeng, A., 2008. Sparse cylindrical sonar arrays. *IEEE J. Ocean. Eng.*, **33**(2):224-231. [doi:10.1109/JOE.2008.923553]

Kirkpatrick, S., Gelatt, C.D., Vecchi, M.P., 1983. Optimization by simulated annealing. *Science*, **220**(4598):671-680. [doi:10.1126/science.220.4598.671]

MathWorks, Inc., 2008. MATALAB 7 Getting Started Guide. Available from http://www.mathworks.com/access/helpdesk/help/pdf_doc/matlab/getstart.pdf [Accessed on Nov. 28, 2008]

Nielsen, R.O., 1991. Sonar Signal Processing. Artech House, Boston, USA, p.51-57.

Palmese, M., Trucco, A., 2007a. Chirp zeta transform beamforming for three-dimensional acoustic imaging. *J. Acoust. Soc. Am.*, **122**(5):EL191-EL195. [doi:10.1121/1.2794881]

Palmese, M., Trucco, A., 2007b. Digital Near Field Beamforming for Efficient 3-D Underwater Acoustic Image Generation. Proc. IEEE Int. Workshop on Imaging Systems and Techniques, p.1-5. [doi:10.1109/IST.2007.379570]

Palmese, M., de Toni, G., Trucco, A., 2006. 3-D Underwater Acoustic Imaging by an Efficient Frequency Domain Beamforming. IEEE Int. Workshop on Imaging Systems and Techniques, p.86-90. [doi:10.1109/IST.2006.1650781]

Spence, T.G., Werner, D.H., 2008. Design of broadband planar arrays based on the optimization of aperiodic tilings. *IEEE Trans. Antenn. Propag.*, **56**(1):76-86. [doi:10.1109/TAP.2007.913145]

Trucco, A., 1999. Thinning and weighting of large planar arrays by simulated annealing. *IEEE Trans. Ultrason. Ferroelectr. Freq. Control*, **46**(2):347-355. [doi:10.1109/58.753023]

Trucco, A., Palmese, M., Repetto, S., 2008. Devising an affordable sonar system for underwater 3-D vision. *IEEE Trans. Instrum. Meas.*, **57**(10):2348-2354. [doi:10.1109/TIM.2008.922111]

van Trees, H.L., 2002. Optimum Array Processing. Part IV of Detection, Estimation, and Modulation Theory. Wiley, New York, p.233-236. [doi:10.1002/0471221104]